Proceedings of the Twenty-eighth (2018) International Ocean and Polar Engineering Conference
Sapporo, Japan, June 10-15, 2018

ISBN 978-1-880653-87-6; ISSN 1098-6189

www.isope.org

Numerical Simulations of Sheet and Cloud Cavitation on NACA0015 with RANS and LES Turbulence Model

Kaijie Chen, Decheng Wan, Gang Chen*

Collaborative Innovation Center for Advanced Ship and Deep-Sea Exploration, State Key Laboratory of Ocean Engineering, School of Naval Architecture, Ocean and Civil Engineering, Shanghai Jiao Tong University, Shanghai, China
*Corresponding Author

ABSTRACT

In the present work, the development of sheet cavitation and the shedding of cloud cavitation around hydrofoil NACA0015 are simulated in RANS and LES method. Three kinds of turbulence models -- SST k-omega, modified SST k-omega and Smagorinsky model are used in this paper. The simulating abilities of sheet and cloud cavitation with those three turbulence models are compared in cavitation shape, shedding frequency and so on. It is found that when simulating at the cavitation number $\sigma = 1$, Smagorinsky and modified SST k-omega turbulence models perform better at the aspects of cavitation shape and shedding frequency. The numerical results also show that the vortex near the wake of sheet cavitation on the suction side is the primary reason for the pinch-off and shedding of sheet cavitation.

KEY WORDS: Cavitation; NACA0015; InterPhaseChangeFoam solver; Large eddy simulation; Modified SST k-omega

INTRODUCTION

Cavitation is a dynamic phase-change phenomenon that often occurs in the flow over rudders, propellers, pumps and other fluid machinery. It is recognized that cavitation occurs when the local pressure drops below the saturated vapor pressure, and collapses in the area where the pressure recovers to large enough, which may lead to several problems such as vibration, erosion and noise on the surface of fluid machinery. Therefore, accurate simulation of cavitation flow becomes more and more significant in the section of propeller design.

The researches on cavitation have been conducted in the last half century. In the early study, experiment was the most effective method which often used stroboscope, pressure sensor and high-speed camera to carry out the prediction in the model scale. Rouse and Mcnown (1948) investigated the cavitation on the cylinders with different head shapes including hemispherical shape, blunt shape, ellipsoidal shape and so on at 0 degree angle of attack . Their cases were introduced as soundness check for cavitation flows by Kunz et al. (2000) and repeated by several authors in the next decades, e.g. Senocak and Shyy (2004), Ahuja et al. (2001) and so on. Kjeldsen et al. (2000) observed the flow around an hydrofoil NACA0015 in a cavitation tube. The results showed that the characteristics of the cavitation are influenced by the angle of attack (AoA) and the cavitation number. Besides, they found that the lift force of the hydrofoil fluctuated violently in a small cavitation number. The case of this hydrofoil at 6 degree angle of attack has been often used as a test case. Amromin et al. (2006) obtained a new hydrofoil OK-2003 by modifying the suction surface of NACA0015 and compared them in experiments. It was found that the cavitation on the suction surface of OK-2003 can effectively reduce the resistance of the hydrofoil, and the amplitude of lift and drag force.

Experimental observations can only give a part of the results due to the limitations in techniques, such as scale effect, inability to consider the impact of the bottom shape of the boat. What's more, this method can't give us the information about the re-entrant jets, which contain the important flow features to study the periodical pinch-off and shedding of the cavitation. Therefore, the access of the complete flow field information through CFD (Computational Fluid Dynamics) would be a popular complement to experimental data.

Early numerical simulations relied on the potential flow methods to model the flow outside the cavitation. The shape of cavitation was determined by the dynamic balance assumptions across the interface between liquid and cavitation. We also called it interface tracking method. This method has the limitations when applied to a flow with vortical structures such as re-entrant jets. So viscous CFD method has been used to model cavitation recently. In this method, the continuity equation is considered with the density varying between vapor and liquid density which determined by the volume fraction of water. In order to model the mass transfer between vapor and liquid, a serials of cavitation models have been applied by different scholars, e.g. Singhal et al. (1997), Merkle et al. (1998), Kunz et al. (2000, 2001) and Sauer et al. (2000). Kim et al. (2009) used SchnerrSauer cavitation model to compare the effect of the turbulence model on the performance of the

cavitation. They pointed out that although RANS, DES and LES had successfully simulated three-dimensional unstable cavitation, such as the oscillation of cavitation and the shedding of cloud cavitation. However, RANS method can not correctly simulate the shedding frequency and predict the lift and drag force. Reboud et al. (1998) gave the results indicating that accurate frequency of the periodical shedding of cavitation can be predicted by an artificial reduction of the turbulent viscosity of RANS.

In this paper, the numerical simulations about two standard test cases -- cylinder with different head shapes and hydrofoil NACA0015 are carried out by interPhaseChangeFoam solver in OpenFOAM with SchnerrSauer cavitation model. SST k-omega turbulence model of RANS and Smagorinsky turbulence model of LES are applied and compared. After finding the better performance of Smagorinsky turbulence model than SST k-omega turbulence model, a serial of modified SST k-omega models are used to artificially reduce of the turbulent viscosity expecting to obtain satisfied results.

NUMERICAL METHOD

Governing Equations

The governing equations for cavitation flow are based on a single phase flow approach, regarding the mixture of fluid and vapor as a single phase whose density can change according to the pressure. The flow field is solved by the mixture continuity and momentum equations plus a volume fraction transport equation to model the cavitation dynamics. As for RANS turbulence model, the equations are presented below.

$$\frac{\partial \rho_m}{\partial t}+\frac{\partial(\rho_m u_j)}{\partial x_j}=0 \tag{1}$$

$$\frac{\partial(\rho_m u_j)}{\partial t}+\frac{\partial(\rho_m u_i u_j)}{\partial x_j}=-\frac{\partial p}{\partial x_j}+\frac{\partial}{\partial x_j}[(\mu_m+\mu_t)(\frac{\partial u_i}{\partial x_j}+\frac{\partial u_j}{\partial x_i})] \tag{2}$$

$$\frac{\partial \alpha_l}{\partial t}+\frac{\partial}{\partial x_j}(\alpha_l u_j)=(\dot{m}^{+}+\dot{m}^{-})/\rho_l \tag{3}$$

The mixture density and the viscosity are defined as follows.

$$\begin{aligned}\rho_m&=\rho_l\alpha_l+\rho_v(1-\alpha_l)\\ \mu_m&=\mu_l\alpha_l+\mu_v(1-\alpha_l)\end{aligned} \tag{4}$$

In the above equations, ρ_l,ρ_v are the liquid and vapor density, α_l,α_v are the liquid fraction and the vapor fraction, μ_t is the turbulent viscosity, $\dot{m}^{+},\dot{m}^{-}$ represent the condensation and evaporation rates. As for LES turbulence model, the momentum equation is modified as follows. τ_{ij} is the subgrid stress (SGS), representing the influence of small scale vortex on the momentum equation.

$$\frac{\partial(\overline{u}_i)}{\partial t}+\frac{\partial(\overline{u}_i\cdot\overline{u}_j)}{\partial x_j}=-\frac{1}{\rho}\cdot\frac{\partial p}{\partial x_j}+\gamma\frac{\partial(2\overline{S}_{ij})}{\partial x_j}-\frac{\partial \tau_{ij}}{\partial x_j} \tag{5}$$

Modified Turbulence Model

Turbulence model plays an important role in the numerical simulation of cavitation flows. The SST k-omega turbulence model which developed by Menter is mixed with the k-omega model in the near-wall area and the k-epsilon model in the far field. Reboud gave the suggestion that an artificial reduction of the turbulent viscosity of this model can predict a more accurate frequency of the periodical shedding of cavitation. So a serial of modified SST k-omega models are applied following his idea.

$$\begin{aligned}\mu_t&=f(\rho)C_\omega\frac{k}{\omega}\\ f(\rho)&=\rho_v+\frac{(\rho_m-\rho_v)^n}{(\rho_l-\rho_v)^{n-1}},n>1\end{aligned} \tag{6}$$

In these modified models,the turbulent viscosity in the area with high vapor volume fraction is reduced so as to better predict the frequency of shedding. The values of *n* in this paper vary from 4 to10.

Mass Transfer Model of SchnerrSauer

The mass transfer model which also called cavitation model adopted here was developed by Schnerr and Sauer. In their papers, the vapor fraction is related to the number of gas nucleus per unit volume and the average radius of gas nucleus. The condensation and evaporation rates are defined as follows

$$\alpha_v=n_0\frac{4}{3}\pi R^3/(n_0\frac{4}{3}\pi R^3+1) \tag{7}$$

$$\begin{aligned}\dot{m}_c&=C_c\frac{3\rho_v\rho_l\alpha_v(1-\alpha_v)}{\rho R}\mathrm{sgn}(P_V-P)\sqrt{\frac{2|P_V-P|}{3\rho_l}}\\ \dot{m}_v&=-C_v\frac{3\rho_v\rho_l\alpha_v(1-\alpha_v)}{\rho R}\mathrm{sgn}(P_V-P)\sqrt{\frac{2|P_V-P|}{3\rho_l}}\end{aligned} \tag{8}$$

R is the average radius of gas nucleus expressed as

$$R=(\frac{\alpha_v}{1-\alpha_v}\cdot\frac{3}{4\pi n_0})^{1/3} \tag{9}$$

The parameter n_0 is the number of gas nucleus per unit volume as an important parameter for the description of mass transfer rates between vapor and fluid. It needs to be provided as input. In this paper, it is set with a default value of 2e+8.

CASE OVERVIEWS

Case of Cylinder with Different Head Shapes

In the last century, a series of experiments were carried out by Hunter Rouse and John S. McNown on the cavitation flow of cylinder with different head forms. A slender cylinder with 1 inch diameter was placed in cavitation tube and the cross-section is perpendicular to the direction of flow. The forms of the upstream head of the cylinder was changed in different cases. They designed a total of three groups of the head shapes. The sensors was set in the surface to obtain the pressure, flow velocity and other parameters. So the cavitation of cylinder with different head shapes in an uniform flow was observed by them.

One group of these cylinders are simulated in this paper, including four models. Fig.1 is one of the models with a hemispherical head. We can consider it as an special case that the chamfer angle is 0.5 D. D represents the diameter of cylinder. So in the other three cases, the

chamfer angles are 0.25 D, 0.125 D and 0 (blunt case).

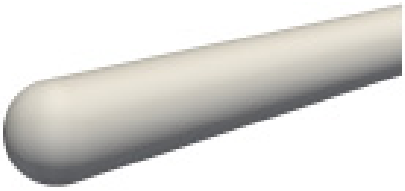

Fig. 1 Model of the cylinder with a hemispherical head shape

First, the cylinder with 0.5D chamfer angle is calculated under three different cavitation numbers (0.2, 0.4 and 0.6).The Reynolds number is 136000. Then the four different models are compared under the same cavitation number (0.4) to validate the solver and determine some cavitation model parameters, such as the number of gas nucleus per unit volume n_0 and the average radius of gas nucleus *dNuc* which are indispensable in our solver. According to these simulations, the preliminary understanding of the mechanism of the developing process of steady cavitation and the relation between the shape of steady cavitation and the cavitation number can be easily got.

The computational domain is -L < X < 3.5 L, -10 D < Y, Z < 10 D, where L is the length of the cylinder and D is the diameter. The inlet velocity is 5.5865 m/s, which is calculated according to the Reynolds number. It must be noted that the characteristic length in this Reynolds number is the diameter of the cylinder, not the length. The pressure gradient and the outlet velocity gradient is zero. The values of inlet pressure corresponding to the cavitation number 0.2, 0.4 and 0.6 are 5866.31 Pa, 8769.24 Pa and 11658.93 Pa. In order to ensure the accuracy of the calculation, the grid is encrypted at four levels outside the surface of the model. The amount of the grid is about 2 million, and the time step is 5e-5s. The simulation domain and the grid are shown in Fig. 2.

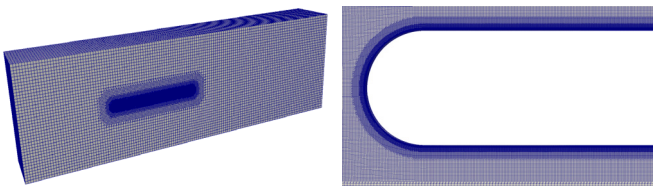

Fig.2 Computational mesh around the cylinder

Case of Hydrofoil NACA0015

NACA0015 is a symmetrical hydrofoil. In this paper, the chord length is 0.2m, and the angle of attack is 6 degrees. Flow velocity is 6m/s. We choose two cases that the cavitation numbers are 1 and 1.6 . According to the relevant documents, when the cavitation number is 1.6, stable sheet cavitation will occur on the suction side which correspond to the area No. III in the Fig. 3. And when the cavitation number is 1, unstable sheet cavitation and cloud cavitation will occur which corresponds to the area No. II. The computational domain is -0.4 m < x <1 m, -0.4 m < y < 0.4 m, and the amount of grid is 4.2 million. Inlet velocity is 6m/s. Pressure gradient and the outlet velocity gradient is zero.

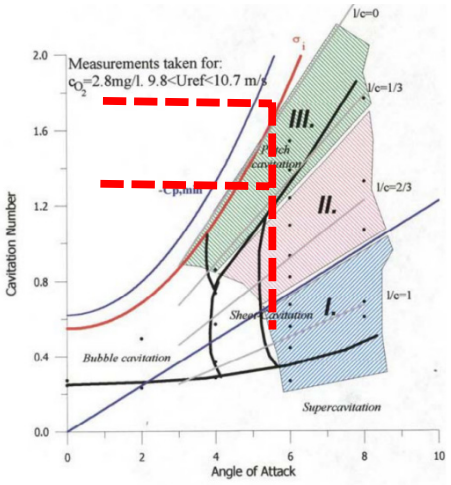

Fig. 3 Cavitation types with different angles of attack and cavitation numbers

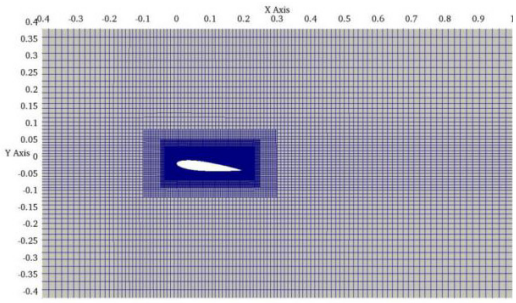

Fig. 4 Computational mesh around the hydrofoil NACA0015

RESULTS AND DISSCUSIONS

Simulation on Cylinder with Steady Cavitation

In order to analyze the pressure distribution on the surface of the cylinder, the dimensionless pressure coefficient is defined.

$$C_p = \frac{p - p_0}{1/2 \cdot \rho \cdot U^2} \tag{10}$$

P is the local pressure of a point on the surface of the cylinder. P_0 represents the pressure in the outlet. The value of U is 5.5865m/s. The pressure distribution of the cylinder with a hemispherical head at the cavitation number 0.4 is shown in Fig. 5.

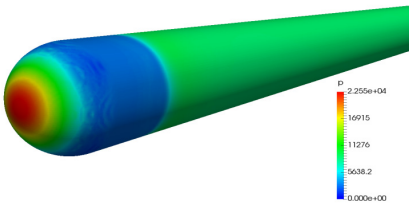

Fig. 5 Pressure distribution of the cylinder with a hemispherical head at the cavitation number 0.4

At the top of the cylinder, due to the collision of flow, the pressure is maximum in the field, and the pressure gradually decreases from the apex to around. When the pressure reduces below the saturated vapor pressure of water, vaporization happens and then the cavitation occurs. In this paper, the value of the saturated vapor pressure of water is 2970 Pa. The area in blue color is the region where cavitation occurs in Fig. 5. Then the cavitation moves backwards, and the pressure restores gradually. When the pressure restores to greater than the saturated vapor pressure, the vapor condenses and turns back to the liquid. The pressure distribution coefficient on the longitudinal section is shown below.

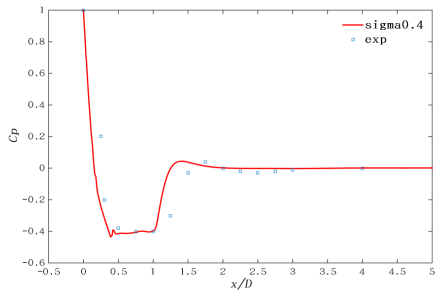

Fig. 6 Pressure coefficient distribution on the longitudinal section

The abscissa represents the dimensionless parameter x/D, while the ordinate represents pressure coefficient. The point whose value in the abscissa is 0 represents the apex of the cylinder. The solid line in red color is the simulation value, and the point in blue color is the experimental value. We can see that the pressure coefficient decreases sharply with the increase of the value in the abscissa at first. When the pressure coefficient reduces to -0.4, cavitation occurs rapidly. Then the pressure coefficient begins to recover when the value in the abscissa increases to approximately 1. We can consider that the section of the solid line that the value of pressure coefficient is -0.4 represents the region where cavitation occurs. The length of the region is about 0.6 D. The graph of pressure distribution coefficient gives us an indirect observation on the cavitation area, while the graph of alpha.water gives a direct approach. The distribution of alpha.water of the simulation and the experiment is shown in Fig. 7, as well as an isosurface of the vapor fraction in Fig. 8. As can be observed, the simulated results agrees well with the experimental data both in the distribution of pressure coefficient and alpha.water.

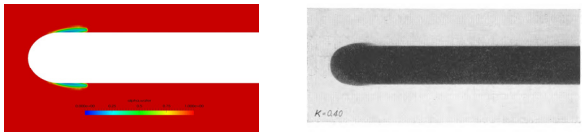

Fig. 7 Distribution of alpha.water of the simulation and the experiment

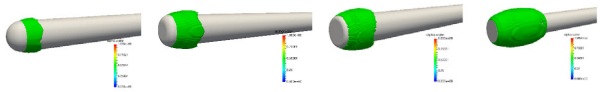

Fig. 8 Cavitation area indicated by an isosurface of the vapor fraction (alpha.water = 0.5)

Then the pressure coefficient in different cavitation numbers is shown in Fig. 9. The simulation results show that the cavitation doesn't occur when the cavitation number is 0.6, which correspond to the conclusion of experiments that the critical value of cavitation number in this case is 0.6. Comparing the lines at cavitation number 0.4 and 0.2, it can be found that the lengths of cavitation area are in a great difference. The former one is 2.6 D while the latter is 0.6 D. It shows that the cavitation numbers have a great influence on the characteristic parameters of cavitation. The smaller the cavitation number, the longer the length of the cavitation. The differences between different head shapes also are shown in Fig.9. The red solid line, the blue solid line, the red dotted line and the green solid line in the right graph in Fig. 9 correspond to four cases that the chamfer radius vary from 0.5D to 0. It can be seen that as the chamfer radius decreases, the length of the cavitation increases. The reason for this phenomenon is that the smaller the chamfer radius, the smaller the collision buffer between the upstream flow and the cylinder. So the amplitude and the area of pressure reduction are really large, and the recovery of pressure becomes hard, which finally lead to the larger length of cavitation.

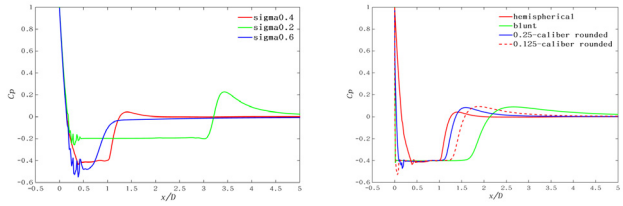

Fig. 9 Pressure coefficient in different cavitation numbers(left) and pressure coefficient with different head shapes(right)

Simulation on NACA0015 in Non-cavitation Flow

Steady non-cavitation flows are computed first to check the grid and the performance in simulating the pressure. It can be seen from Fig. 10 that when the flow is divided by the hydrofoil, there is a low pressure area on the suction side of the hydrofoil and a high pressure area at the font of the pressure side. There is also a slightly local high pressure region at the tail part of the hydrofoil.The distribution of pressure coefficient is also shown in Fig. 10 and compared with Li et al. (2009).

The simulated pressure distribution is consistent with the results calculated by Li et al. in *Fluent*. The values of high pressure point, low pressure point and slightly high pressure point at the tail part are also consistent with Li et al. In addition, the results of lift coefficient and drag coefficient are also satisfied, which are shown in Table 1. It shows that the simulation results in wet flow of NACA0015 calculated by OpenFOAM are reliable in the detail information of flow fields.

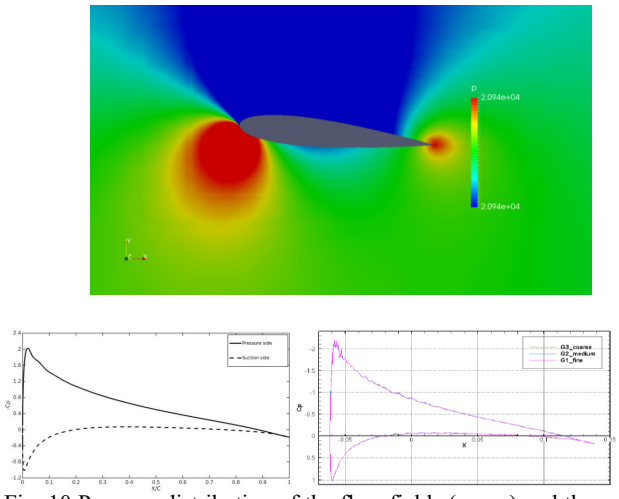

Fig. 10 Pressure distribution of the flow fields (upper) and the pressure coefficient on the surface of NACA0015 of this paper (lower left) and Li et al. (lower right)

Table 1. Lift and drag coefficient in non-cavitation flow

	Value of simulation	Value of Li et al.	Difference
C_L	0.651	0.660	-1.36%
C_D	0.0143	0.014	2.14%

Simulation on NACA0015 in Cavitation Flow with SST k-omega Model

All the simulations in RANS method are carried out with SST k-omega turbulence model. At the condition that the cavitation number is 1.6, the partial sheet cavitation occurs on the suction side of the hydrofoil shown in Fig. 11. The cavitation is tightly attached to the surface of the object and there is no obvious shedding. The cavitation is considered to be steady.

As for the condition that cavitation number is 1, the cavitation becomes unsteady. We can observe the obviously periodical change in the shape of cavitation, as shown in Fig. 12. Analyzing the shape of cavitation at different time, we can see the periodical process as follows. First, because of the collision between flow and hydrofoil, there is a region where the pressure is below the saturated vapor pressure, so the fluid evaporates abruptly and forms the cavitation which like a piece of sheet attached on the hydrofoil. Then, the sheet cavitation grows up until it is pinched off by the re-entrant jet. Afterwards, the section of cavitation which is pinched off moves backward while the re-entrant jet flows to the area ahead. Therefore, the re-entrant jet collides with the incoming flow and cloud cavitation appears because of the sheering action during the collision. Finally, the cloud cavitation moves backward with the incoming flow and disappears gradually, while the sheet cavitation of the next period occurs on the front of the suction side.

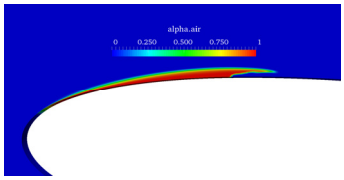

Fig.11 Steady cavitation indicating by alpha.water when cavitation number is 1.6

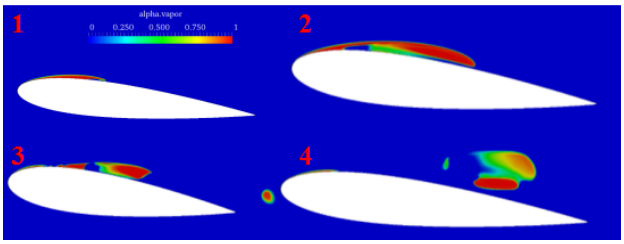

Fig. 12 Periodical change in the shape of cavitation when cavitation number is 1

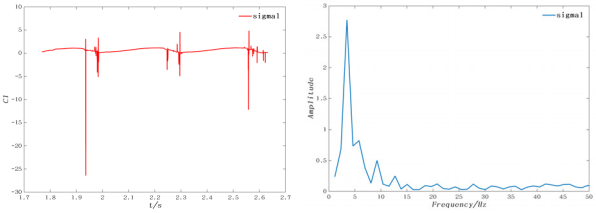

Fig.13 Lift coefficient curve and the shedding frequency of cavitation by fast Fourier transform

According to the curve of lift coefficient, we can obtain the shedding frequency of cavitation by fast Fourier transform (FFT). The results are shown in Fig. 13. It can be seen from the figure that the main frequency of the shedding is 3.469Hz.

Simulation on NACA0015 in Cavitation Flow with LES

The simulations in LES method are carried out with Smagorinsky turbulence model. The cavitation number in the simulation is 1 and the physical density ratio is used with $\rho_l / \rho_v = 66500$. The ratio of the span and the chord is infinitely large in order to avoid the influence of the side face of the hydrofoil. The shapes of cavitation are shown in Fig. 14. Compared with the case in RANS method, this case can predict more accurate shape of cloud cavitation. After the pinch-off of sheet cavitation and the collision between the incoming flow and the re-entrant jet, there will be much more cloud cavitation with defferent size of bubble on the suction side in a very large region. The LES method models this phenomenon successfully, while in the results of RANS method with SST k-omega turbulence model only a little area of cloud cavitation with large size of bubble can be observed. Besides, the shedding frequency is 11.2 Hz according to the lift and drag coefficient curve shown in Fig. 15, which is much bigger than the case with SST k-omega model.

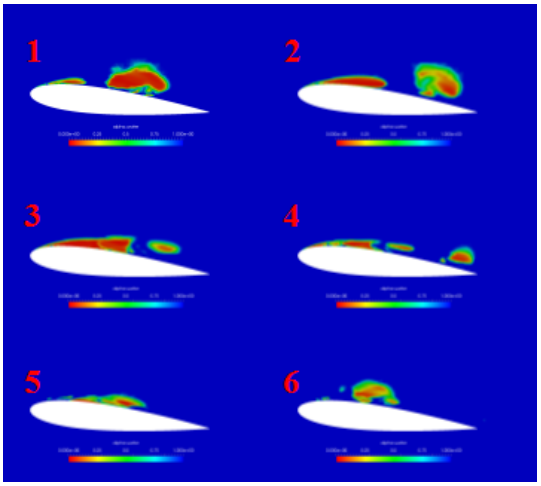

Fig. 14 Cavitation in LES method with Smagorinsky turbulence model

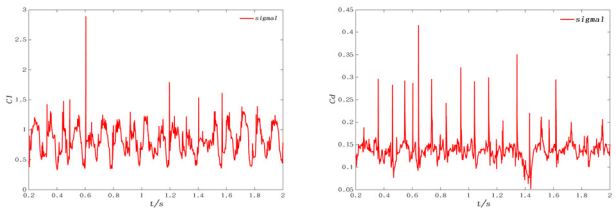

Fig.15 Lift and drag coefficient of NACA0015 in LES method

Simulation on NACA0015 in Cavitation Flow with Modified SST k-omega Model

Reboud et al. (1998) gave the results indicating that accurate frequency of the periodical shedding of cloud cavitation can be predicted by an artificial reduction of the turbulent viscosity of RANS. Therefore, a modified SST k-omega model is applied in this case. The modified model is different from the SST k-omega model in the formula of nut, which represents the turbulent viscosity, as defined in Eq. 6. Because of the artificial reduction of the turbulent viscosity, the shedding of cavitation becomes easier and the frequency is much larger than the results with SST k-omega model. Fig. 16 shows the periodical change of cavitation with modified SST k-omega model in which the value of n is 10. n is an artificial parameter to define the modified SST k-omega model as mentioned in Eq. 6. Fig. 17 shows the lift coefficient curve with different values of n which can give us the information about the shedding frequency, and the corresponding frequencies are 14.98Hz, 6.08 Hz and 4.28 Hz.

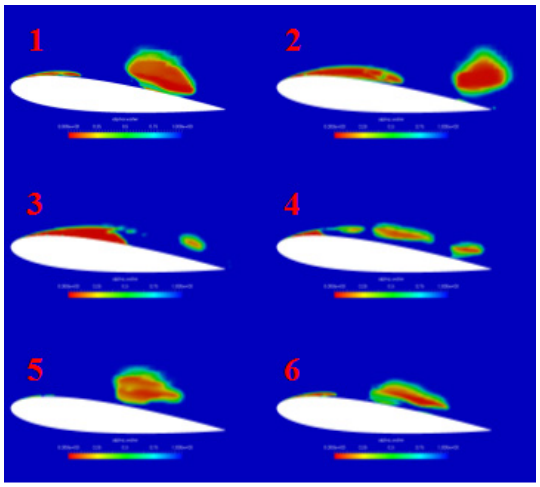

Fig. 16 Periodical change in the shape of cavitation with modified SST k-omega model

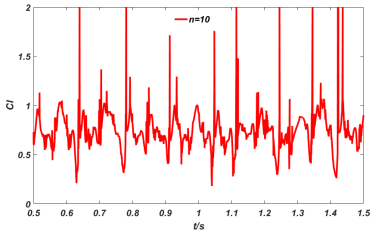

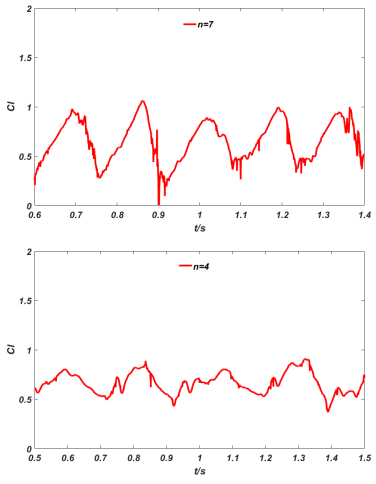

Fig.17 Lift coefficient of NACA0015 with modified SST k-omega model at different n (n=10, 7, 4 in order)

Comparison on Three Kinds of Turbulence Model

Three kinds of turbulence model are used above -- SST k-omega model, Smagorinsky turbulence model and modified SST k-omega model. The results about the shedding frequency of all cases with these three kinds of turbulence models are shown in Table 2 together and compared with the data from other authors. It is found that the modified SST k-omega model gives best performance on predicting the shedding frequency when the value of n set as 10. Smagorinsky model also predicts a slightly large value of the frequency, while the SST k-omega model and modified SST k-omega model with n = 4, 7 do not perform well. In fact, the SST k-omega model correspond to the special case when the value of n is 1 in the modified SST k-omega model. In other words, the results with modified SST k-omega model are unsatisfactory when n = 1, 4, 7. So the value of n is suggested to set as 10 to obtain good results of shedding frequency.

Besides,comparing Fig. 12, Fig. 14 and Fig. 16, it can be found that Smagorinsky and modified SST k-omega model perform much better than SST k-omega model in modeling the shape of cavitation during the periodical change, especially the period of shedding. In the corresponding figures of the Smagorinsky and modified SST k-omega model, we can obviously observe the shedding from the sheet cavitation several times not only one or two times, and we can see that several bubbles with cloud shape exist at the same time in different region of the suction side, while the same phenomenon can't be observed in Fig.12.

Table 2. Summary of shedding frequencies

	Frequency (Hz)
RANS, SST k-omega model (special modified model when n=1)	3.47
LES, Smagorinsky model	11.20
RANS, modified SST k-omega model , n = 10	14.98
RANS, modified SST k-omega model , n = 7	6.08

RANS, modified SST k-omega model , n = 4	4.28
Hoekstra and Vaz (2008)	15.4
Oprea (2009)	14

Analysis about the Mechanism of periodical change in Cavitation

The diagrams about velocity vector of the flow fields are shown in Fig. 18. Analyzing the velocity vector diagram, it's found that vortex structure occurs in the tail region during the growth of sheet cavitation. After that, the flow which is perpendicular to the wall in the vortex structure pinches off the sheet cavitation. Then there will be a margin area between cavitation and wall, so re-entrant jets appear in this region with a contrary direction to the incoming flow and collides with the incoming flow which leads to the cloud cavitation due to the sheering action during the collision. Therefore, the vortex is the primary reason for the shedding of sheet cavitation.

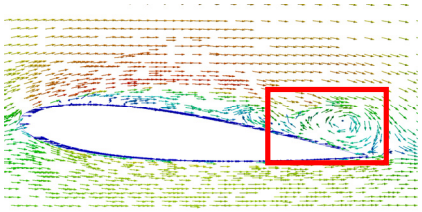

(a) Vortex structure

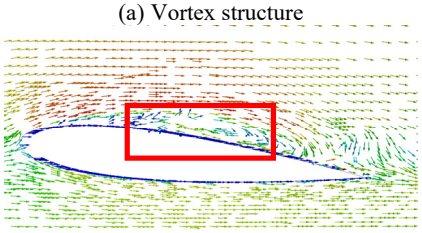

(b) Re-entrant jets

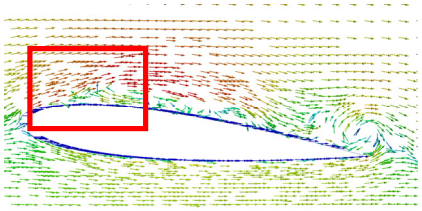

(c) Collison between re-entrant jets and incoming flow

Fig. 18. Velocity vector of the flow fields at different time

CONCLUSIONS

The paper presents the numerical simulations about two standard test cases -- cylinder with different head shapes and hydrofoil NACA0015 by interPhaseChangeFoam solver in OpenFOAM with SchnerrSauer cavitation model. SST k-omega model, Smagorinsky turbulence model and modified SST k-omega model are applied in different cases. The numerical results of cavitation shape indicating by alpha.water, shedding frequency, lift and drag coefficient are compared with different turbulence models. It is found that SST k-omega model can predict the steady cavitation around the cylinder and the steady sheet cavitation on NACA0015 at the cavitation number $\sigma = 1$, but it doesn't simulate well on the unsteady cavitation. So, it is necessary to use LES method or modifying the turbulence model in RANS method to obtain the accurate simulation about unsteady cavitation. Both Smagorinsky model and modified SST k-omega model give relatively good results compared with SST k-omega model, while the modified SST k-omega model even performs more satisfied than Smagorinsky model in LES method. Therefore, the modified SST k-omega model is recommended. The periodical change in the shape of cavitation with those models can be concluded as follows. First, the fluid evaporates abruptly in the low pressure region and forms the cavitation which like a piece of sheet attached on the hydrofoil. Then, the sheet cavitation grows up until it is pinched off by the re-entrant jet and the re-entrant jet flows to the area ahead colliding with the incoming flow causing much of cloud cavitation appearing because of the sheering action during the collision. The numerical results also show that the vortex structure in the tail region on the suction side is the primary reason for the shedding of the cavitation.

ACKNOWLEDGEMENTS

This work is supported by the National Natural Science Foundation of China (51490675, 11432009, 51579145), Chang Jiang Scholars Program (T2014099), Shanghai Excellent Academic Leaders Program (17XD1402300), Program for Professor of Special Appointment (Eastern Scholar) at Shanghai Institutions of Higher Learning (2013022), Innovative Special Project of Numerical Tank of Ministry of Industry and Information Technology of China (2016-23/09) and Lloyd's Register Foundation for doctoral student, to which the authors are most grateful.

REFERENCES

Ahuja, V, Arunajatesan, S, and Hosangadi, A (2001). "Simulations of Cavitating Flows Using Hybrid Unstructured Meshes," *Journal of Fluids Engineering*, 123(2), 331-340.

Amromin, E, Kopriva, J, Arndt, REA, and Wosnik, M (2006). "Hydrofoil Drag Reduction by Partial Cavitation," *Journal of Fluids Engineering*, 128(5), 931-936.

Coutierdelgosha, O, Astolfi, JA (2003). "Numerical Prediction of the Cavitating Flow on A Two-dimensional Symmetrical Hydrofoil With A Single Fluid Model," *5th Int. Symp. on Cavitation*, Osaka, Japan.

Huang, B, Wang, G, Yuan, H (2010). "A cavitation model for cavitating flow simulation," *Journal of Hydrodynamics*, 22(5), 798-804.

Kim, SE (2009). "A numerical study of unsteady cavitation on a hydrofoil," *Proceedings of the 7th international symposium on cavitation*, Ann Arbor, Michigan, USA.

Kjeldsen, M (2000). "Spectral Characteristics of Sheet and Cloud Cavitation." *Journal of Fluids Engineering*, 122(3), 481-487.

Kunz, RF, Boger, DA, Chyczewski, TS, Stinebring, DR, Gibeling, HJ, and Govindan, TR (2000). "A preconditioned Navier-Stokes method for two phase flows with application to cavitation prediction," *Computers and Fluids*, 29(8), 849-875.

Medvitz, RB, Kunz, RF, Boger, DA, Lindau, JW, Yocum, AM, and Pauley, LL (2002). "Performance analysis of cavitating flow in centrifugal pumps using multiphase CFD," *Journal of Fluids Engineering*, Transactions of the ASME, 124(2), 377-383.

Merkle, CL, Feng, J, and Buelow, PEO (1998), "Computational modeling of the dynamics of sheet cavitation," 3*th International Symposium on Cavitation*, Grenoble, France.

Rhee, S, Kawamura, T, Li, H (2003). "A study of propeller cavitation using a RANS CFD method," *8th international conference on numerical ship hydrodynamics*, Busan, Korea.

Rouse, H, and Mcnown, JS (1948). "Cavitation and pressure distribution: Head forms at zero angle of yaw." *Proactive Maintenance for Mechanical Systems*,169–191.

Schnerr, GH, and Sauer, J (2001). "Physical and Numerical Modeling of Unsteady Cavitation Dynamics," *Proc. 4th International Conference on Multiphase Flow*, New Orleans, USA.

Senocak, I, and Shyy, W (2001). "Numerical Simulation of Turbulent with Sheet Cavitation," *4th International Symposium on Cavitation*, Pasadena, USA.

Senocak, I, and Shyy, W (2004). "Interfacial dynamics-based modelling of turbulent cavitating flows, Part-1: Model development and steady-state computations." *Frontiers in Public Health*, 2(2), 141.